Crop Adaptation and Migration to Climate Change in the MENA and Mediterranean Regions

Adrian Kreiner [a], Kanishka Mallick [b], Aolin Jia [b], Tian Hu [b], Abdelhakim Amazirh [c], Zoltan Szantoi [a]

a) European Space Agency, Frascati 00044, Italy
b) Luxembourg Institute of Science and Technology, Belvaux 4362, Luxembourg
c) Mohammed VI Polytechnic University, Marrakesh, Morocco

Introduction

The Middle East and North Africa (MENA) and the Mediterranean region are facing increasing heat and drought risks due to climate change [1], severely threatening its rainfed agriculture production [2]. Agricultural systems adapt to climate change through in-situ strategies (adjusting planting dates, heat-tolerant cultivars, irrigation) and crop migration (shifting growing regions). This study analyzes how crops adapt to increasingly frequent drought conditions in arid and semi-arid regions (2004-2024), examining drought patterns using diurnal land surface temperature measurements from Meteosat Second Generation to create thermal indicators that serve as soil moisture deficit proxies.

Study Area

The analysis focuses on the irrigated and rainfed agricultural areas within semi-arid and arid regions of MENA and the Mediterranean regions.

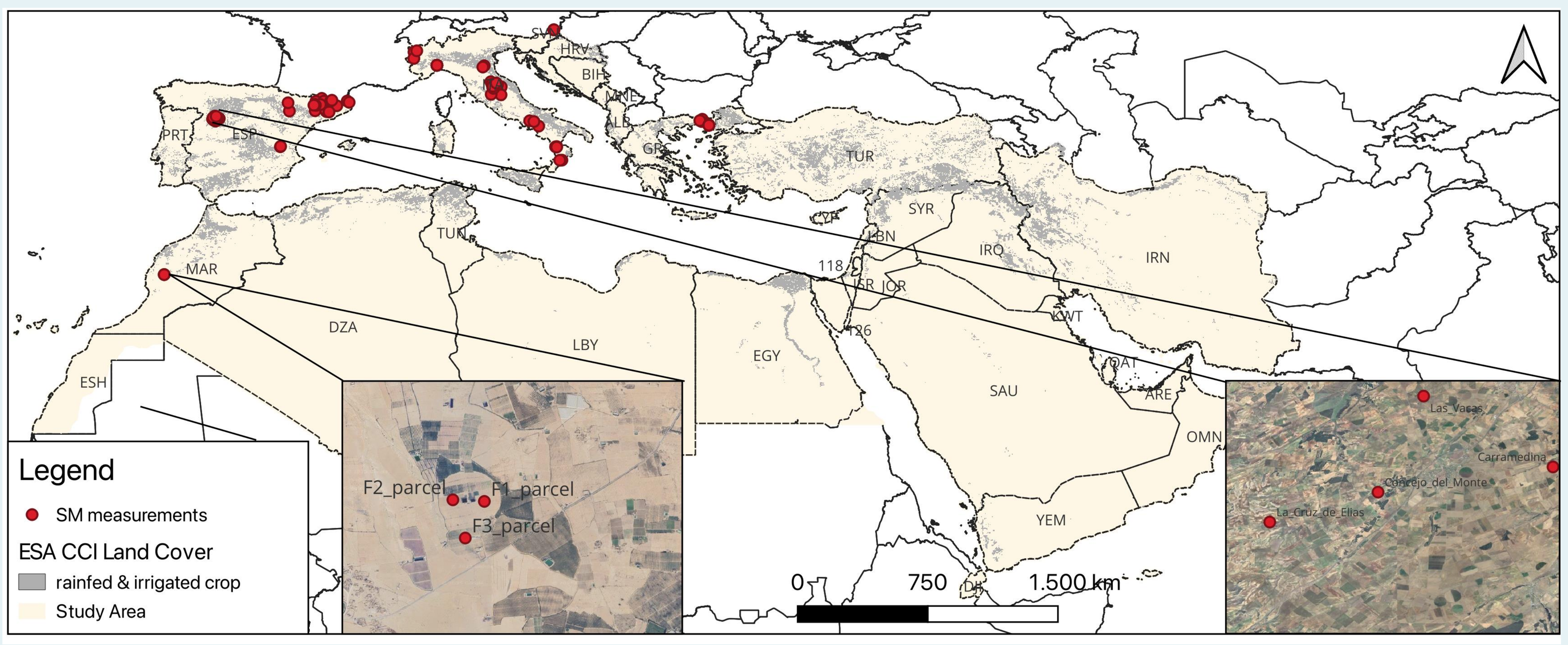

Figure 1: Study area and stable cropland (2004–2022) from ESA CCI Land Cover. Soil moisture measurements from International Soil Moisture Network (ISMN) and [3] (black)

Drought Indicator

Several indicators were tested against in situ soil moisture. Temperature Rise Index (TRI) [5] (clear/all-sky) and Aparent Thermal Inertia [6] showed limited consistency and were not selected. Selected indicators include dLST (Eq. 1) and Radiative Thermal Inertia (RTI) (Eq. 2) using daily radiation sum. RTI variants using maximum shortwave or shortwave at time of max LST, and clear- vs. all-sky conditions, showed poorer performance. RTI accounts for the energy needed to raise surface temperature by 1 K and the correction factor (e^{RH}) corrects for vegetation damping effects to improve spatial applicability [7]. A third indicator based on hourly LST–air temperature difference (Eq. 3) [8] is planned for future testing.

$$(1)\ dLST = LST^{all-sky}_{max,d} - LST^{all-sky}_{min,d}$$

$$(2)\ RTI = \frac{(1-\alpha)R_S^{\downarrow} + \varepsilon R_L^{\downarrow}}{dLST_{min,\,max}} * e^{RH}$$

$$(3)\ LST - T_a = \sum (LST_h - T_{a,h})$$

$LST^{all-sky}_{min,d}$ = daily all-sky min. land surface temp. [K]
$R_S^{\downarrow}, R_L^{\downarrow}$ = daily sum of downward, shortwave/longwave radiation [J/m²]
α, ε = albedo [-], emissivity [-]
RH = relative humidity [-]
$T_{a,h}$ = hourly air temperature [K]

Methods

To assess crop adaptation through **in-situ adaptation** or **migration**, we analyze changes in several **drought indicators** across **agricultural areas** during the **vegetation period**. First, we compare these indicators to in-situ soil moisture data and EO products. Second, we analyze the drought indicators over time using a **weighted quantile regression method,** where each crop is weighted by **Gross Primary Production (GPP)** to reflect productivity differences. This methodology (Figure 2) follows a counterfactual approach, comparing:

1. **Observed scenario**: Actual shifts in weighted crop areas over time from 2004 to 2024.
2. **Counterfactual scenario**: Weighted crop areas were kept constant in their 2004-2010 average distribution.

As the drought indicator changes over time (t1 → t2), crop areas may:

- Shift to regions with more favorable moisture conditions (migration),
- Remain stable despite changes in TRI (in situ adaptation), or
- Decrease overall or niche expansion

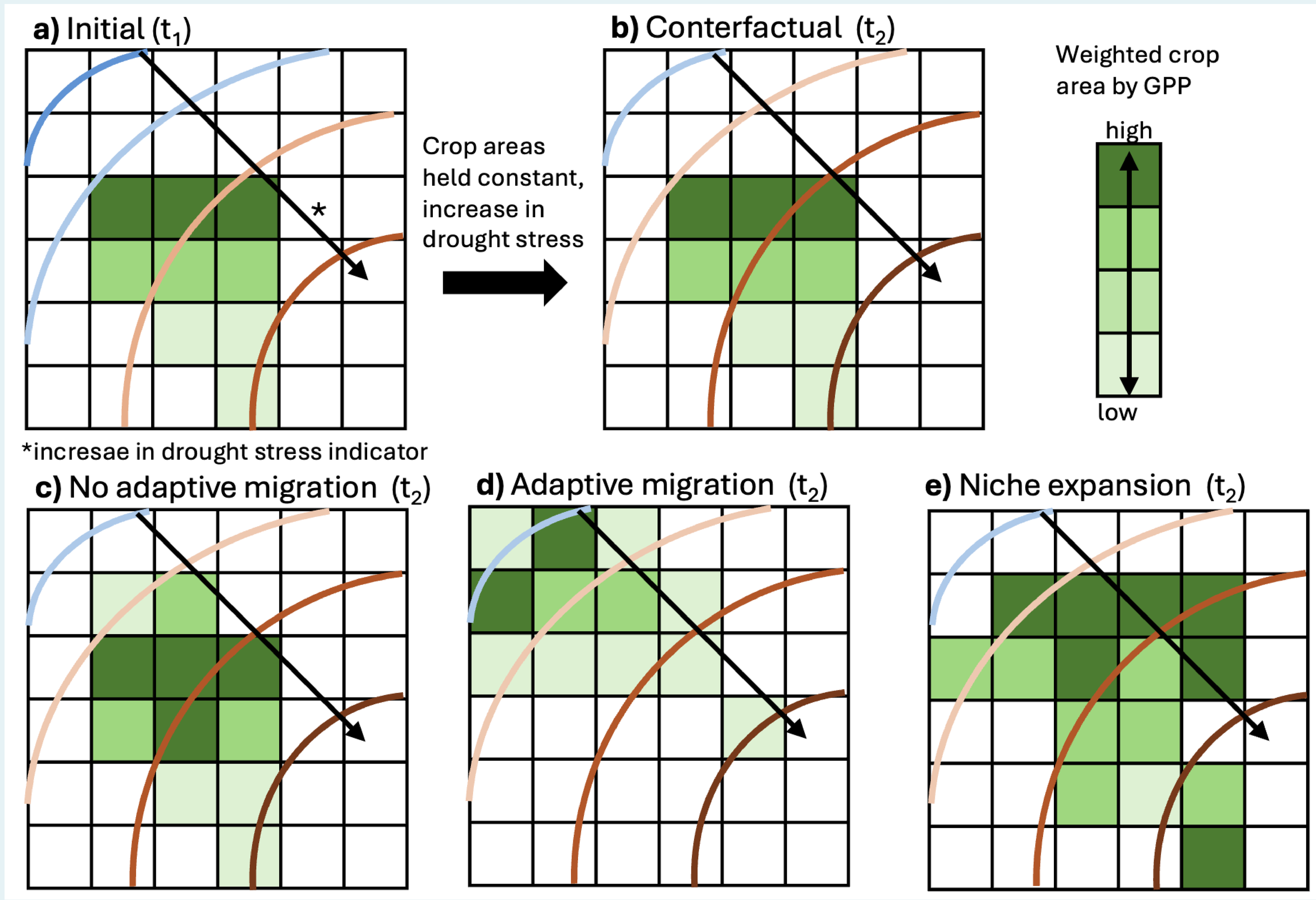

Figure 2: Panels (a–e) illustrate theoretical crop distribution changes, where darker green represents higher weighted crop areas (weighted by GPP). (a) represents the initial period (t_1), while (b–e) depict scenarios at a later time (t_2) as drought indicator changes. Comparing observed vs. counterfactual (fixed) weighted crop areas reveals adaptation patterns: no difference e.g. in the 95th percentile trend means no migration, a lower trend suggests migration to cooler areas, and a higher trend indicates expansion into warmer regions. Illustration adapted from [4].

LST all-sky data and radiation data (30 min, 0.05°) are from LSA SAF derived from the Meteosat Second Generation geostationary satellite. Crop areas are identified using ESA CCI Land Cover. Vegetation season timing is derived from MODIS MCD12Q2 (v6.1) and GPP from MODIS MOD17A2HGF.061. Relative humidity is calculated from ERA5-Land.

Results & Discussion

The drought indicators dLST and RTI, especially when corrected with relative humidity, showed the highest correlation with in situ soil moisture (up to 35 cm depth) on a weekly basis across stations (e.g., Fig. 3 & 4). TRI, based on early morning temperature rise (1.5–3.5 h after sunrise) showed lower correlation due to the fact that the time period is too short and does not fully capture the temperature increase.

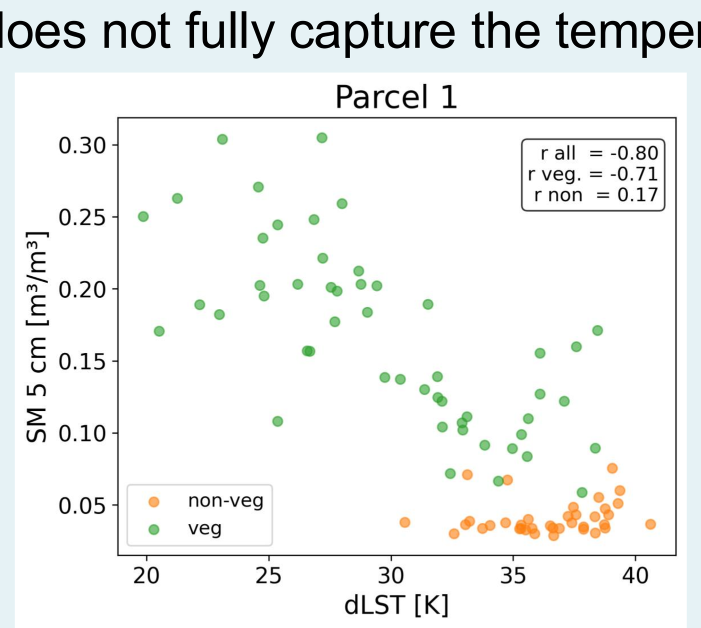

Figure 3: Correlation between dLST and soil moisture at the F1 Parcel during the vegetation period (2017/2018), weekly.

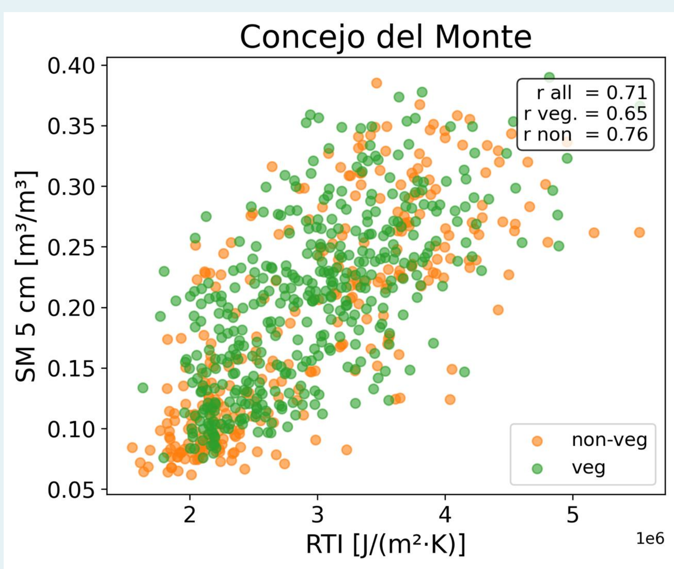

Figure 4: Correlation between RTI and soil moisture at the Concejo del Monte station during the veg. period (2004–2024) weekly.

MODIS-based analysis (2004–2023) showed that 24.6% of stable rainfed crop pixels experienced a significant shift in season start (mean: –1.24 days/year), and 23.8% in season end (–0.59 days/year), highlighting crop calendar shifts as a key adaptation mechanism.

At the Concejo del Monte station, weekly dLST anomaly trends (2004–2024) indicate a cooling trend early in the season—possibly due to increased irrigation—and warming in later stages, suggesting rising drought stress. These are preliminary findings; future work will scale this analysis to regional level using all three drought indicators.

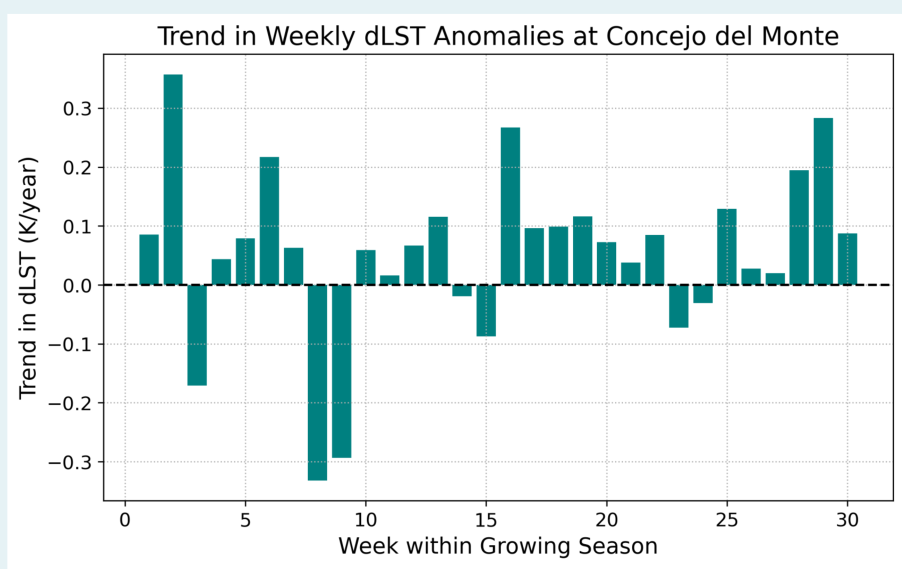

Figure 5: Trend in weekly dLST anomaly during the growing season at Concejo del Monte (2004–2024), based on a 2004–2010 baseline.

References

1. Namdar et al. (2021). Climate change and vulnerability in MENA. *ISPRS Int. J. Geo-Inf.*, 10(11):794.
2. Li et al. (2025). Climate change impacts on crop yields and food security. *Sci. Rep.*
3. Ouaadi et al. (2021). Monitoring wheat in semi-arid Morocco with C-band radar. *Earth Syst. Sci. Data*, 13, 3707–3731.
4. Sloat et al. (2020). Crop migration as climate adaptation. *Nat. Commun.*, 11(1):1–9.
5. Hu et al. (2020). Monitoring drought with MTSAT-2 LST in Australia. *Remote Sens. Environ.*, 236, 111419.
6. van Doninck et al. (2011). MODIS apparent thermal inertia for soil moisture. *Int. J. Appl. Earth Obs.*, 13(6), 934–941.
7. Jia et al. (in press). High-res drought index using ECOSTRESS LST.
8. Cai et al. (2025). Sub-diurnal LST–air temp anomaly for drought detection in Australia. *Remote Sens. Environ.*, 327.